Cancer Letters 457 (2019) 86–97

Contents lists available at ScienceDirect

Cancer Letters

journal homepage: www.elsevier.com/locate/canlet

Original Articles

Targeting the Shc-EGFR interaction with indomethacin inhibits MAP kinase pathway signalling

Chi-Chuan Lin[a], Kin Man Suen[a,b], Amy Stainthorp[a], Lukasz Wieteska[a], George S. Biggs[c], Andrei Leitão[d], Carlos A. Montanari[d], John E. Ladbury[a,e,*]

[a] School of Molecular and Cellular Biology, University of Leeds, Leeds, LS2 9JT, UK
[b] Wellcome Trust Cancer Research UK Gurdon Institute, University of Cambridge, Tennis Court Road, Cambridge, CB2 1QN, UK
[c] Department of Chemistry, University of Cambridge, Lensfield Road, Cambridge, CB2 1EQ, UK
[d] Medicinal Chemistry Group (NEQUIMED), São Carlos Institute of Chemistry, University of São Paulo (IQSC-USP), 13566-590, São Carlos, SP, Brazil
[e] Department of Chemistry, Indian Institute of Technology Bombay, Powai, Mumbai, 400076, India

ARTICLE INFO

Keywords:
Shc PTB domain
Erk signalling
Therapeutic repurposing
Mechanism of action

ABSTRACT

Receptor tyrosine kinase (RTK)-mediated hyperactivation of the MAPK/Erk pathway is responsible for a large number of pathogenic outcomes including many cancers. Considerable effort has been directed at targeting this pathway with varying degrees of long term therapeutic success. Under non-stimulated conditions Erk is bound to the adaptor protein Shc preventing aberrant signalling by sequestering Erk from activation by Mek. Activated RTK recruits Shc, via its phosphotyrosine binding (PTB) domain (Shc^{PTB}), precipitating the release of Erk to engage in a signalling response. Here we describe a novel approach to inhibition of MAP kinase signal transduction through attempting to preserve the Shc-Erk complex under conditions of activated receptor. A library of existing drug molecules was computationally screened for hits that would bind to the Shc^{PTB} and block its interaction with the RTKs EGFR and ErbB2. The primary hit from the screen was indomethacin, a non-steroidal anti-inflammatory drug. Validation of this molecule *in vitro* and in cellular efficacy studies in cancer cells provides proof of principle of the approach to pathway down-regulation and a potential optimizable lead compound.

1. Introduction

Receptor tyrosine kinase (RTK) signalling is initiated by the binding of an extracellular growth factor. Through a variety of RTK-related idiosyncratic mechanisms, this event results in up-regulation of kinase activity, auto-phosphorylation and recruitment of downstream effector proteins to phosphorylated tyrosine residues. In normal differentiated tissue, cells are not persistently exposed to activating concentrations of growth factors. As a result there is the potential for redundancy of RTKs and their associated downstream signalling proteins. Despite this these proteins are maintained at relatively high concentration in the plasma membrane and cytoplasm respectively. To prevent aberrant signal transduction by the available signalling molecules the cell has to impose rigorous control mechanisms. One such mechanism requires the sequestering of a key member of the mitogen-activated kinase (MAPK) signalling pathway, Erk (extracellular-regulated kinase), by the adaptor protein Shc (Src homology 2-containing transforming protein). As part of this complex Erk is prevented from being recruited to its upstream activating kinase Mek (MAPK/Erk kinase), thus ensuring signal transduction is abrogated in the absence of stimulation [1].

Shc is an adaptor protein which, despite possessing no intrinsic catalytic activity, plays an integral part in signal transduction pathways that are perturbed in several different cancers [2,3]. The p52 isoform of Shc (henceforth referred to simply as Shc) comprises an N-terminal phosphotyrosine-binding domain (PTB, henceforth referred to as Shc^{PTB}), a collagen homology 1 (CH1) domain and a C-terminal Src homology 2 (SH2) domain. In stimulated cells Shc has been shown to play a role in linking RTKs to the MAPK pathway [4–6]. Post-stimulation phosphorylation of the RTK provides a phosphotyrosine (pY) residue-containing site (bearing the consensus sequence NPXpY, where X is any amino acid [4]). Shc is recruited to this site through its PTB domain [7–10]. Subsequent phosphorylation of tyrosine residues (Y239. Y240 and Y317) on the CH1 domain of Shc promotes the recruitment of another adaptor protein, growth factor receptor binding protein (Grb2 [11,12]). The concomitant Shc-mediated localization of Grb2 induces complex formation with the guanine nucleotide exchange

* Corresponding author. School of Molecular and Cellular Biology, University of Leeds, Leeds, LS2 9JT, UK.
E-mail address: j.e.ladbury@leeds.ac.uk (J.E. Ladbury).

https://doi.org/10.1016/j.canlet.2019.05.008
Received 22 March 2019; Received in revised form 9 May 2019; Accepted 10 May 2019

factor, Sos, and represents the key initiating event in MAPK signalling. This is followed by up-regulation of Ras and Raf and ultimately results in the phosphorylation of Erk by Mek [13,14]. The MAPK pathway can also be activated via direct interaction of Grb2 with RTKs followed by recruitment of Sos. Although, this mode of pathway stimulation circumvents Shc mediation, we have previously demonstrated that the sequestration of Erk through binding to Shc was sufficient to inhibit Erk phosphorylation and response [1].

As the terminal kinase in the MAPK pathway, Erk plays a fundamental role in transducing signals from growth factor-stimulated RTKs to induce cell growth, survival and differentiation. Prolonged phosphorylation of Erk results in cell proliferative signals, as a result Erk is found upregulated in many forms of cancer, including ovarian [15], prostate [16] and Hodgkin's disease [17]. Activated Erk functions as a serine-threonine kinase directed towards numerous substrate proteins [18–20]. In its activated state it also translocates to the nucleus to stimulate transcription of specific genes [13,21]. Erk can also regulate the MAPK pathway through negative feedback inhibition [22]. Furthermore, Erk is involved in cross-talk with other pathways which are usurped in cancer [23,24]. Erk has two functionally and structurally similar isoforms, Erk1 and Erk2 (henceforth communally referred to as Erk).

Previously we demonstrated that Shc is a key negative regulator of MAPK signalling in non-stimulated cells. Shc forms a complex which sequesters Erk from involvement in MAP kinase signalling [1]. The binding site for Erk is situated on the Shc^{PTB} distal from the pTyr binding site. Recruitment of Shc on RTK up-regulation results in the adaptor protein undergoing a conformational change that releases Erk. Free Erk is then available to be recruited, phosphorylated and hence activated by Mek. In the context of constitutively up-regulated RTKs, the loss of Shc regulation of Erk could be a contributing factor in exacerbating oncogenic phenotypes, thus we reasoned that a molecule that can block Shc binding to activated RTKs without triggering the release of Erk would be beneficial in the treatment of Erk-dependent cancers (Fig. 1A). Not only would such an inhibitor sustain the Shc-Erk complex, but it is also anticipated that prohibition of Shc^{PTB} binding to the receptor would also prevent phosphorylation of tyrosine residues on the CH1 domain and abrogate the binding of Grb2, hence blocking Ras activation. Thus, discovery of an appropriate molecule will provide a dual function inhibitor. This approach is validated by, for example, the observation that disabling Shc^{PTB} in mice can lead to delayed tumour onset [25].

Initially an *in silico* docking screen was used to select small molecule candidates directed at the Shc^{PTB} for the inhibition of Shc-RTKs interaction. Our approach to this was to use an established database of known drug compounds (DrugBank [26]) to assess whether potential hits could provide an opportunity for repurposing. We discovered that indomethacin, a known non-steroid anti-inflammatory drug (NSAID), interacts with the Shc^{PTB} directly *in vitro*. We employed biophysical methods and NMR to investigate the interaction at the molecular level and demonstrate that the indomethacin-Shc^{PTB} interaction binds in the canonical phosphotyrosine-binding pocket without disruption of the Erk-binding site. We further show that in cells treated with indomethacin the drug competes with phosphorylated EGFR (epidermal growth factor receptor) for binding to Shc, and in doing so is able to down-regulate Erk signalling in a panel of cancer cell lines. This study provides validation of the approach of inhibiting Shc binding to RTKs as a promising therapeutic strategy as well as highlighting the possibility of developing indomethacin-like compounds as leads to inhibit Erk activity.

2. Materials and methods

2.1. Cheminformatics approach

The chemical structures of the approved drugs were retrieved from the DrugBank database and prepared using the set of programs from OpenEye Software. The fixpka tool from QUACPAC software (1.7.0.2: OpenEye Scientific Software, Santa Fe, NM) was applied to ionize the chemical groups at neutral pH. Then two hundred conformations were generated with Omega (v. 3.0.0, OpenEye Software, Santa Fe, NM) for all novel compounds (henceforth all other parameters kept as default will not be mentioned) [27]. The NMR structure of the Shc^{PTB} domain (PDB code: 1SHC [7]) was chosen to dock putative novel ligands into the pocket. The protein structure was prepared with the Make Receptor tool for docking in the OEDocking suite (v. 3.2.0, OpenEye Software, Santa Fe, NM) [28–30]. The box volume was 24,468 $Å^3$ with the following dimensions; 26.0 Å × 23.33 Å x 40.33 Å, having inner and outer volumes of 23 $Å^3$ and 15118 $Å^3$ respectively. The use of the balanced potential provided the surface around the peptide ligand binding site in which the inner volume was positioned around the aromatic ring of the pTyr in the structure. Two constraints were imposed due to the high importance of the electrostatic interactions: (i) a carboxylic acid should fit in the sphere placed on the phosphorous atom of the phosphate group; (ii) one hydrogen bond acceptor should be pointing towards the Arg175. The docking software FRED was applied with the Chemgauss4 scoring function to rank the compounds. Images were generated using Chimera v. 1.12 [31] and PoseView [32] on line (http://poseview.zbh.uni-hamburg.de/).

2.2. Cell culture

All cells were maintained in Dulbecco's modified Eagle's high glucose medium (DMEM) supplemented with 10% (v/v) foetal bovine serum (FBS) and 1% antibiotic/antimycotic (Lonza) in a humidified incubator with 10% CO_2.

2.3. Reagents

Antibodies for pErk (4695), Erk (4377), pY317 Shc (2431), pY1148 EGFR (4404), EGFR (2646), Tubulin (2144) were obtained from Cell Signalling Technology; Shc (06–203) was from Millipore. Normal mouse IgG (sc-2025), agarose-conjugated Shc antibody (SC-967 AC), agarose-conjugated EGFR antibody (SC-120 AC), and protein A/G plus-agarose (sc-2003) were from Santa Cruz Biotechnology. Recombinant Human EGF Protein, CF (236-EG) was from R&D systems. Indomethacin (I7378) was from Sigma-Aldrich, all indomethacin analogues were from ChemBridge Corporation.

2.4. Cloning, expression and purification of recombinant proteins

Prokaryotic expression plasmid for Shc^{PTB} domain has been described previously [1]. Shc^{PTB} R175Q was generated using site-direct mutagenesis. Histidine-tagged fusion proteins were purified from BL21(DE3) cells. A single colony was used to transform 100 ml of LB which was grown overnight at 37 °C. 1 L of LB were inoculated with 10 mL of this overnight culture and were allowed to grow at 37 °C until the OD_{600} = 0.8 at which point the culture was cooled down to 20 °C and expression was induced with 1 mM IPTG. Cultures were allowed to grow for a further 12 h before harvesting by centrifugation. Cells were re-suspended in 20 mM Tris, 150 mM NaCl, 10% glycerol, pH 8.0 in the presence of protease inhibitors and lysed by sonication. Insoluble material was removed by centrifugation (13,000 g at 4 °C for 60 min). The soluble fraction was applied to a Talon column. Following a wash with 10 times column volume of buffer (20 mM Tris, 150 mM NaCl, pH 8.0) protein was eluted from the column with 150 mM imidazole and was concentrated to 5 mL and applied to a Superdex75 gel filtration column in buffer containing 20 mM HEPES, 150 mM NaCl and 1 mM TCEP pH 7.5. Analysis of pure proteins on SDS-PAGE showed greater than 98% purity.

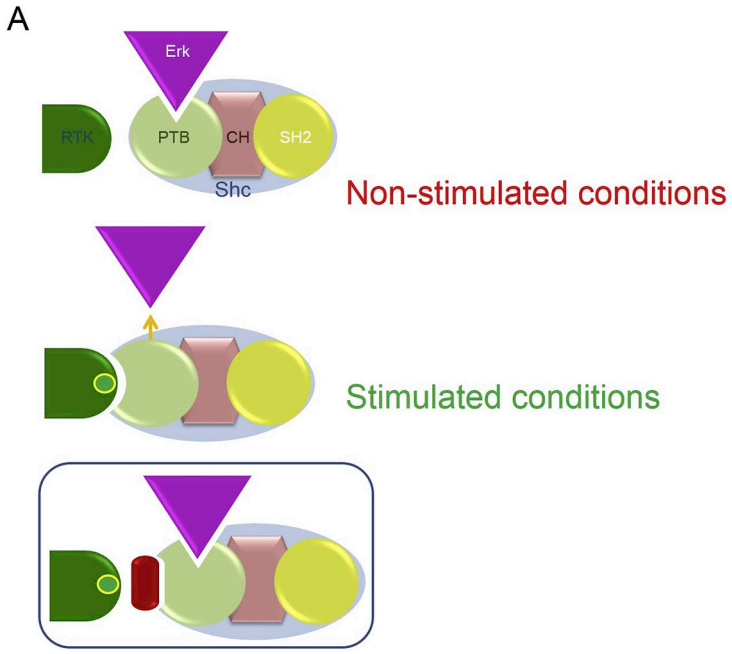

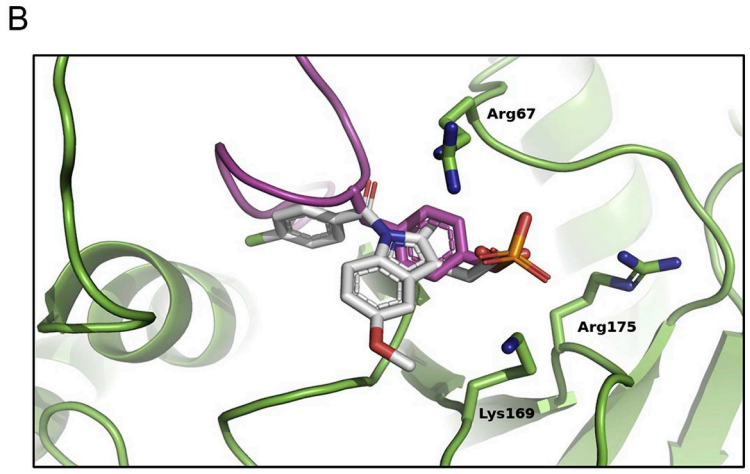

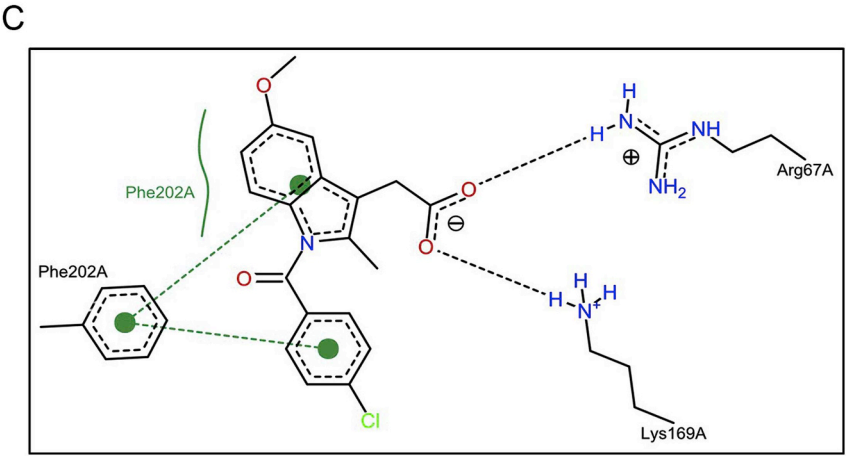

Fig. 1. Compound identification from *in silico* screen of DrugBank library. (A) Schematic of the mode-of-action of the proposed inhibitor. Top panel: Non stimulated state. Shc (blue oval with binding domains overlaid) binds to Erk, sequestering it from possible recruitment by the MAPK signalling pathway. Middle panel: Stimulated state. Shc is recruited by the RTK. On binding to the phosphorylated tyrosine (green/yellow dot) Erk is released and can join the MAPK pathway. Bottom panel: Stimulated state. The inhibitor (red lozenge) blocks the binding of Shc to the receptor leaving Erk bound to Shc and hence inaccessible to MAPK signalling. (B) Superimposition of indomethacin (grey carbons) and the phosphopeptide (pink carbons) in the PTB binding site of Shc (green ribbons); (C) The two-dimensional representation of the intermolecular interactions for indomethacin. The side chain and identification of the positive amino acids that surround the phosphate at the pocket are also depicted in (B). Images were generated using Chimera v. 1.12 [38] and PoseView [39] on line (http://poseview.zbh.uni-hamburg.de/).

2.5. Indomethacin treatment and cell lysates

Indomethacin was prepared as 1 M stock in DMSO. For cell based studies, cells were serum starved in the presence of different concentrations of indomethacin overnight. All cells were viable after serum starvation, i.e. we found no evidence of cell death. 10 ng/ml EGF was used to stimulate cells for 2 or 5 min. Following PBS washing, cells were lysed with lysis buffer containing 50 mM HEPES (pH 7.5), 0.1% (v/v) NP-40, 10 mM NaF, 1 mM sodium orthovanadate, 10% (v/v) glycerol, 50 mM NaCl, 1 mM PMSF and Protease Inhibitor Cocktail Set III (Calbiochem) and required concentrations of indomethacin as indicated. Cell debris was removed by centrifugation at 13,000 rpm for 20 min. The detergent soluble fraction was used for western blotting or immuneprecipitation experiments. The cells which are marked as having zero indomethacin have only the experimental level of DMSO added and thus act as a control for the effects of the solvent.

2.6. Immunoprecipitation and western blots

For immunoprecipitation experiments, cells were lysed with lysis buffer as described above and 0.5 mg of whole cell lysate was prepared in 500 µL volume. IP antibody was added to the lysate and incubated overnight. The beads were then spun down at 4000 rpm for 3 min, supernatant was removed and the beads were washed with 1 ml lysis buffer. This washing procedure was repeated five times in order to remove non-specific binding. After the last wash, 50 µl of 2× Laemmli sample buffer were added, the sample was boiled and subjected to SDS-PAGE and western blot assay.

For western blotting cells were grown in 10 cm dishes, serum starved overnight and stimulated with 10 ng/ml EGF for the indicated time period. Cells were lysed using lysis buffer as described above. For immunoblotting, proteins were separated by SDS-PAGE, transferred to PVDF membranes and incubated with the specific antibodies. Immune complexes were detected with horseradish peroxidase conjugated secondary antibodies and visualized by enhanced chemiluminescence reagent according to the manufacturer's instructions (Pierce).

2.7. Microscale thermophoresis (MST)

The binding affinities were measured using the Monolith NT.115 (NanoTemper Technologies, GmbH). Shc^{PTB} was fluorescently labelled with Atto488 according to the manufacturer's protocol. Labelling efficiency was determined to be 1:1 (protein:dye) by measuring the absorbance at 280 and 488 nm. A 16 step dilution series of the unlabelled binding partner (indomethacin) was prepared in a 2% DMSO solution, mixed with the labelled protein at 1:1 ratio and loaded into capillaries. Measurements were performed at 25 °C in 20 mM HEPES, 150 mM NaCl and 1 mM TCEP pH 7.5 buffer containing 0.01% Tween 20 and 2% DMSO. Data analyses were performed using Nanotemper Analysis software, v.1.2.101, and were plotted using Origin 7.0. All measurements were conducted as triplicates and the errors were presented as the standard error of the triplicates.

2.8. Isothermal titration calorimetry (ITC)

ITC experiments were carried out using a MicroCal iTC200 (Malvern) or VT ITC at 25 °C. Twenty 15 µl injections of 1400 µM indomethacin were made into 140 µM Shc PTB in the calorimeter cell. Control experiments involving the injection of 1400 µM indomethacin into buffer or buffer into 140 µM Shc^{PTB} were performed. The heat per injection was determined and subtracted from the binding data. Data were analysed using a single independent site model using Origin software.

For the Shc^{PTB} binding to phospho-EGFR and phosphor-ErbB2 peptides experiments, twenty 2 µl injections of 500 µM peptides were titrated into 50 µM Shc^{PTB}. Shc^{PTB}-indomethacin complex was prepared by pre-incubation of 50 µM Shc^{PTB} with 2 mM indomethacin.

Indomethacin was prepared as a 1 M stock solution in 100% DMSO and diluted to desired concentration with 2% DMSO final concentration.

2.9. Nuclear magnetic resonance spectroscopy (NMR)

NMR acquisitions were carried out in the NMR buffer (20 mM HEPES, 100 mM NaCl, 0.5 mM TCEP and 10% (v/v) D_2O) for the 190 µM ^{15}N uniformly labelled Shc^{PTB}. A BEST version [33,34] of amide transverse relaxation optimized spectroscopy (TROSY) [35] pulse sequence was used to record amide NMR spectra. All measurements were recorded at 25 °C on a 950 MHz Brücker spectrometer equipped with a Brücker TCI triple-resonance cryogenically cooled probe. Data was processed with NMRPipe [36] and analysed with CcpNmr Analysis software packages [37]. Stepwise addition of the selected drugs led to chemical shifts for several resonances. To characterize ligand binding chemical shift perturbation was applied. Euclidean distance moved was calculated using formula with the scaling factor $\alpha = 0.04$. Calculated distances > 0.02 ppm were considered as significant. Peak assignments of Shc^{PTB} backbone ^{15}N resonances were obtained from Biological Magnetic Resonance Data Bank (Entry ID 17080).

2.10. Wound healing assay

A431 cells were serum-starved overnight by which time confluence reached about 80%. An artificial homogenous wound was made onto the monolayer using an IncuCyte® 96-well WoundMaker Tool. After wounding debris was removed by washing cells with PBS. Serum-depleted medium containing 800 µM of indomethacin or the same volume of DMSO were added to the wounded cells and 100 ng/ml of EGF ligand was added to each well. At different time points cells that migrated into the wounded area or cells with extended protrusions from the wound border were photographed using IncuCyte Live-Cell Analysis.

3. Results

3.1. Identification of small molecules for Shc PTB by in silico docking

We performed an *in silico* screen of approved drug compounds from the DrugBank database [27] to identify potential hits directed at the pTyr binding site on the Shc^{PTB}. This pocket is highly positively charged to accommodate the tyrosyl phosphate of the cognate RTK. The available structure of pTyr bound to Shc^{PTB} reveals that pTyr is placed the electron-deficient pocket in Shc^{PTB} surrounded by three basic amino acids (Arg67, Arg175 and Lys169) which make strong electrostatic interactions [7]. The computational model was built to capture the same chemical environment to dock the drugs into the PTB domain of Shc (Fig. 1B). The DrugBank drug compounds were evaluated to attribute charges for the basic and acid groups at neutral pH. Before analysis, fatty acids, amino acids, polycarboxylated compounds and compounds with multiple charges were identified and excluded from the study. Drugs having one carboxylic acid moiety were prioritized in the knowledge that this chemical group is a bioisostere of the phosphate on tyrosylphosphate-containing ligands.

The most promising drug for further studies was selected using an approach comprising the weighted Chemgauss4 score (dividing the score value by the molecular weight of the compound). Bearing in mind that some molecules presented poses with almost no overlap with the native ligand, the intermolecular interactions and pose in comparison with the native ligand were also considered in the analyses. After an analysis of the top scored compounds indomethacin, a known NSAID, was found to be the best virtual hit optimizing interactions with both Arg67 and Lys169 on the Shc^{PTB} structure (Fig. 1C). Indomethacin sits in the heart of the pTyr binding site with a similar intermolecular interaction pattern that was observed for the native ligand in the target pocket.

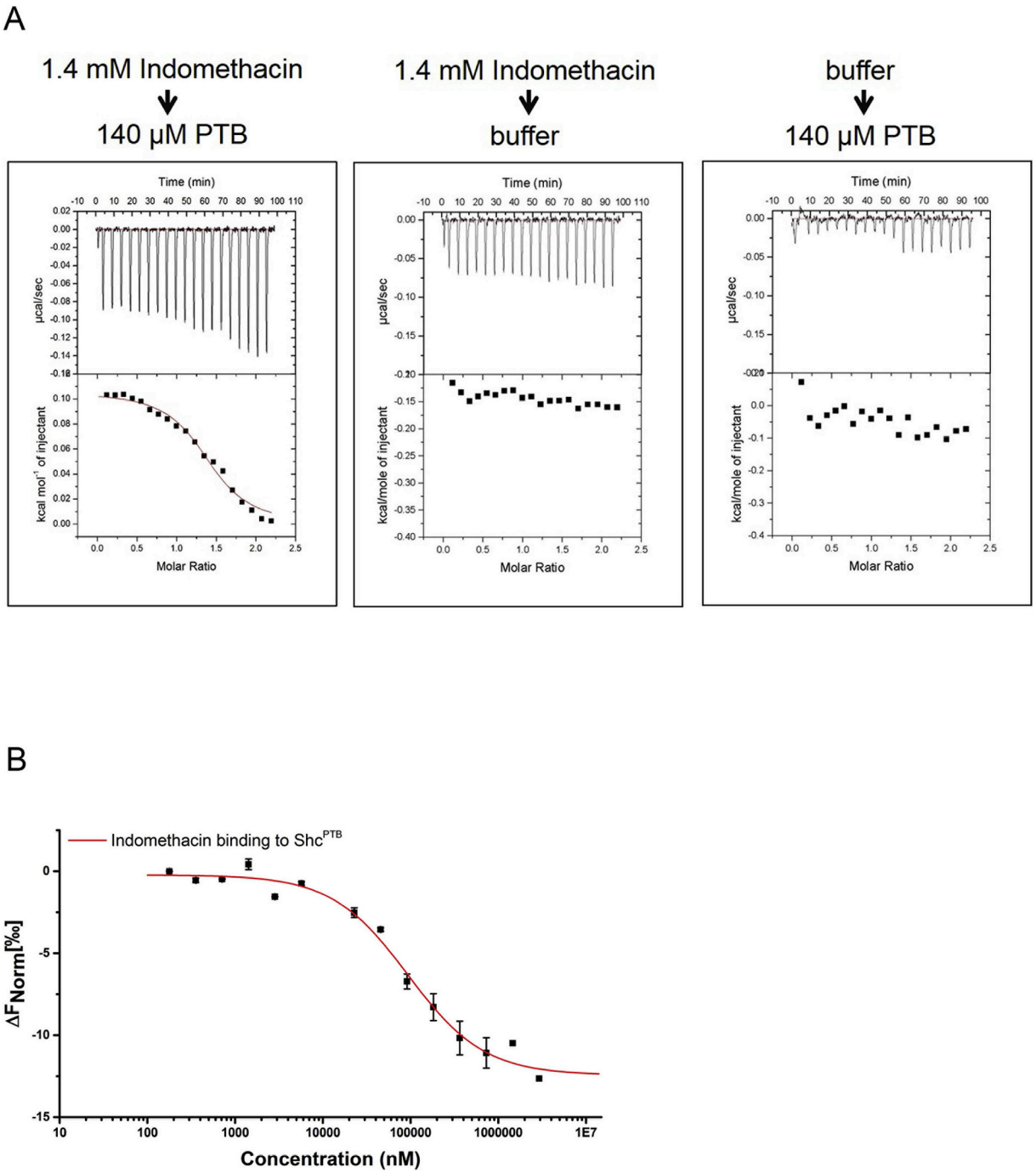

Fig. 2. Direct interaction of indomethacin and Shc^{PTB}. (**A**) ITC measurement of the interaction between Indomethacin and Shc^{PTB}. Left: Twenty 15 μl injections of indomethacin (1400 μM) were titrated into Shc^{PTB} (140 μM) at 25 °C. Top panel: baseline-corrected power versus time plot for the titration. Bottom panel: the integrated heats and the molar ratio of the indomethacin to Shc^{PTB}. Middle: the heats of dilution of 1400 mM indomethacin titrated into buffer. Right: the heats of dilution of buffer titrated into Shc^{PTB} (140 μM). (**B**) Interaction of indomethacin with Shc^{PTB} is measured using MST. Unlabelled indomethacin (2.9 μM–178 nM) was titrated into a fixed concentration of labelled Shc^{PTB} (50 nM).

3.2. Indomethacin binds to the phosphotyrosine-binding pocket of the Shc^{PTB} domain

Both isothermal titration calorimetry (ITC) and microscale thermophoresis (MST) were used to determine the affinity of the interaction between the recombinant Shc^{PTB} and indomethacin (K_d = 38.2 ± 7.2 μM; Fig. 2A K_d = 93.6 ± 5.6 μM; Fig. 2B respectively). The unfavourable enthalpic contribution to binding (positive ΔH; Fig. 2A) suggests that the binding of the drug is driven by the change in entropy (ΔS) implicating the release of water molecules from apolar surface in the binding site as an important energetic contribution to interaction. This observation is supported by the presence of Phe202 that, in our docking model, interacts with the hydrophobic surfaces of the indole and chlorobenzoyl groups in indomethacin (Fig. 1C). We failed to observe binding amongst a range of indomethacin analogues and carboxylic acid-containing compounds suggesting that the pTyr-Shc^{PTB} binding site exhibits some selectivity for indomethacin (Supplementary Fig. 1).

Having shown that indomethacin and the Shc^{PTB} interact directly, we endeavoured to ascertain whether the interaction between

indomethacin and the Shc^{PTB} is indeed via the pTyr binding pocket as predicted *in silico*. Initially, 2D [^{1}H, ^{15}N] NMR spectroscopy was used to identify the indomethacin binding site in the Shc^{PTB}. This was achieved by performing a titration of indomethacin into the Shc^{PTB} and measuring the changes in chemical shifts for ^{1}H and ^{15}N atoms. Chemical shift perturbation (CSP) is the result of a change in local chemical

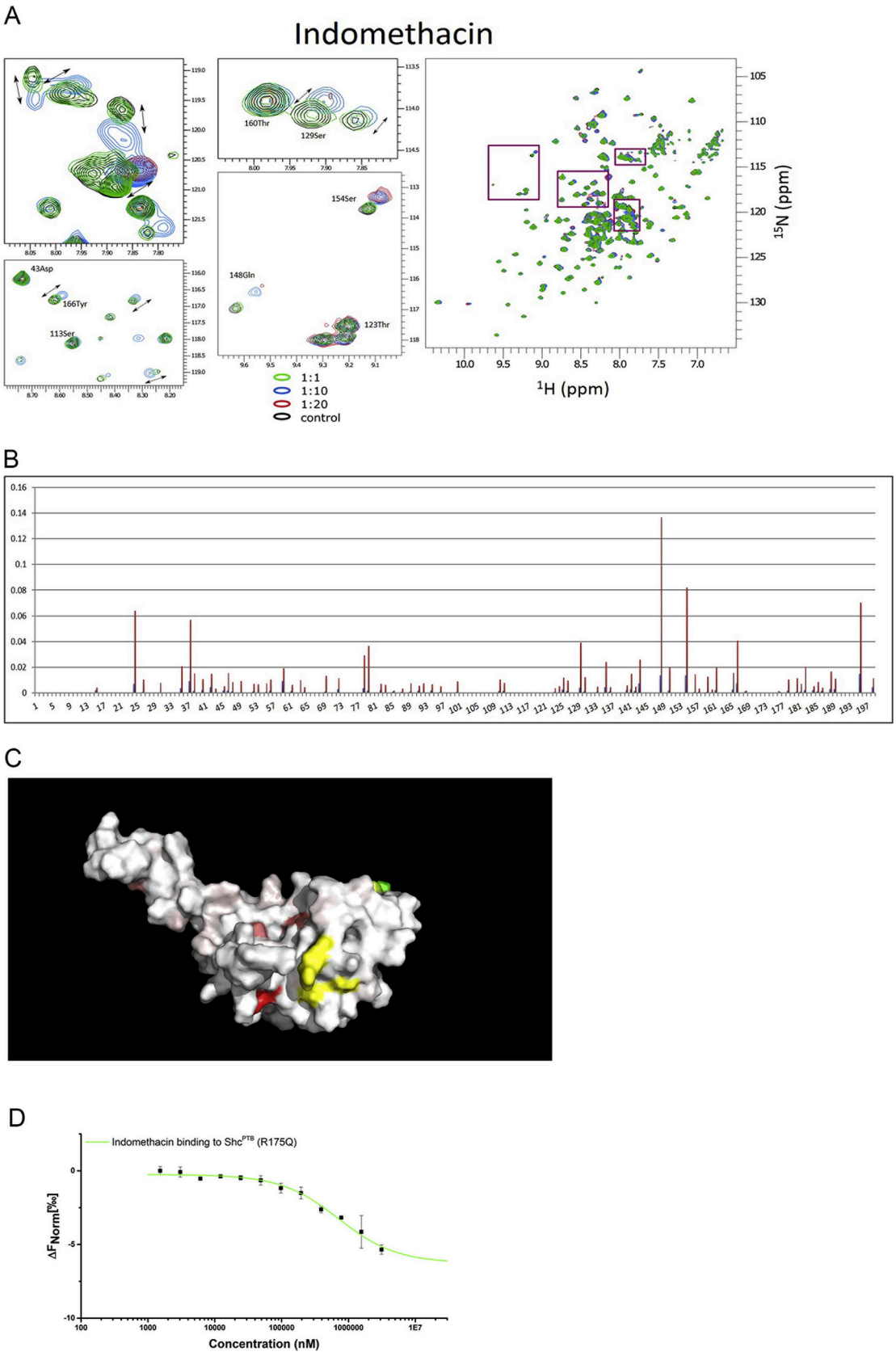

(caption on next page)

Fig. 3. Characterization of the indomethacin- Shc^{PTB} interaction. (**A**) Sections of the ^{1}H–^{15}N HSQC spectra of Shc^{PTB} showing indomethacin binding-induced chemical shift changes. Arrows indicate the peak movement. The unbound peaks are in black and the final bound (1:20) peaks are in red. (**B**) Plot of the chemical shift changes (ppm) of the backbone amide peaks of ^{15}N-labelled Shc^{PTB} upon addition of 1 molar equivalent of indomethacin and 10 molar equivalent of indomethacin. (**C**) Chemical shift perturbations of residues (> 0.03 ppm) from plot in (B) mapped on the NMR structure of the Shc^{PTB} (PDB code: 1SHC). The colour gradient from salmon pink to red indicates the strength of the perturbation (ppm) of specific residues. The critical residues in the pTyr binding pockets are coloured in yellow (R67, K169, and R175). The image shows that putative binding region with localized higher perturbation is proximal to the pTyr binding pocket. Residues in green correspond to the Erk binding site. (**D**) Interaction of indomethacin with mutant Shc^{PTB} (R175Q) measured using MST. Unlabelled indomethacin (2.9 nM–178 nM) was titrated into a fixed concentration of labelled Shc^{PTB} (50 nM).

environment of the atom which can be linked to the presence of a ligand in the complex. Stepwise addition of indomethacin led to CSPs for several Shc^{PTB} backbone ^{15}N resonances. (Fig. 3A and B, Supplementary Fig. 2). As expected for a ligand with moderate affinity the chemical shift changes are not pronounced, however clear shifts are observable for some atoms. Attributing these to residues in the PTB domain and mapping these onto the structure (Fig. 3C), shows that the region that experiences the largest perturbation includes that proximal to the pTyr binding site incorporating Lys169 which is expected to hydrogen bond with indomethacin (Fig. 1C). Indeed, the largest shift is seen for Gln148 which points toward the pTyr binding site. Importantly, the binding of indomethacin appears to be located distally from the Erk binding site suggesting that binding of the drug would not impinge on the sequestering of Erk by Shc (Fig. 3C). By way of comparison we analysed the 2D [^{1}H, ^{15}N] NMR spectral data collected for other commercially available indomethacin-like compounds; 1-(4-fluorobenzyl)-5-methoxy-2-methyloindole-3-acetic acid (Supplementary 3A and 3B) and indomethacin heptyl ester (Supplementary 3C and 3D). It is clear from the plots of CSP derived from these two compounds that the impact on the Shc^{PTB} structure is negligible. This suggests further that within the indomethacin analogues there is selectivity for this site.

To confirm that indomethacin binds in the pTyr binding pocket we mutated an arginine residue in the Shc^{PTB} binding site, which is essential for pTyr recognition, to the polar glutamine (Arg175Gln). The reduction of the affinity by approximately an order of magnitude (K_d = 590 ± 54 μM; Fig. 3D) demonstrates that indomethacin, like the pTyr cognate ligand requires the presence of Arg175. Although Arg175 does not appear to sustain the interaction in the original screening model, this amino acid is placed at 4.2 and 4.4 Å respectively away from the charged groups of indomethacin. This distance falls within the range of a salt bridge interaction and hence could stabilize the positioning of the carboxylic acid group on indomethacin.

3.3. Indomethacin competes with RTK for binding of Shc^{PTB}

The efficacy of indomethacin as an inhibitor of binding of Shc^{PTB} to RTKs is dependent on its ability to compete for binding to Shc with the tyrosyl phosphate site on the receptor. The Shc^{PTB} has been shown to directly interact with phosphorylated tyrosine residues on the EGFR family RTKs EGFR (aka. ErbB1; human epidermal growth factor receptor binding protein 1) and ErbB2 upon stimulation by EGF [38–40]. ITC was used to provide a qualitative assessment of whether the binding of cognate pTyr-containing peptides could be inhibited by the presence of indomethacin. Peptides corresponding to the amino acid sequences around pTyr1148 (EGFR peptide: STAVGNPEpYLNT) on EGFR, and pTyr1122 (ErbB2 peptide: SPAFDNLYpYWDQ), a proposed binding site on ErbB2, were synthesized and 500 μM of each was titrated into 50 μM of Shc^{PTB} in the absence, or the presence of 2 mM indomethacin (Fig. 4A and B). The binding of the Shc^{PTB} to the peptides is low affinity, however the changes in observed heat measured, when compared to the control experiment of buffer into PTB domain, reveal that binding occurs. The isotherms obtained also show that when the Shc^{PTB} is pre-saturated with indomethacin the binding is reduced or abrogated altogether. Using MST we could measure the binding of Shc^{PTB} to ErbB2 pTyr1122 in the absence and presence of indomethacin. As with the ITC experiment in the absence of the small molecule binding was observed (K_d = 261 ± 50.7 nM), however after saturation no binding was apparent (Fig. 4C).

3.4. Indomethacin down-regulates EGF-dependent Erk pathway in cancer cell lines

The *in vitro* experimental data to date validate the *in silico* docking model and demonstrate that indomethacin binds with moderate/low affinity and occupies the pTyr-binding site within the Shc^{PTB}. These data also confirm that indomethacin can prevent the recruitment of Shc^{PTB} to activated RTKs, and hence potentially prolong the sequestering of Erk from MAPK signalling. To explore this we used cell-based assays to assess how downstream signalling might be affected by the inhibitory presence of indomethacin. A panel of cell lines which express Shc were serum-starved overnight in the presence of indomethacin at varying concentrations. Cells were then stimulated with 10 ng/ml EGF for 2 min. Amongst the cell lines we chose two breast cancer cell lines, MCF7 and SkBr3, due to the strong link between Shc expression status and breast cancer progression. We also tested carcinoma cell lines derived from skin (A431), kidney (A498) and cervix (HeLa). The effects of indomethacin on EGFR signalling were examined by immunoblotting. In all cell lines we used, the phosphorylation of Erk upon EGF stimulation was down-regulated upon indomethacin treatment (Fig. 5).

Examination of the signalling events that occur upstream of Erk revealed two discrete mechanisms. In the first mechanism (represented by SkBr3, Fig. 5B and A498, Fig. 5D) the MAPK pathway is up-regulated on addition of EGF leading to phosphorylation of Mek which is independent of the concentration of indomethacin added. However, the level of pErk is reduced in a dose-dependent way, suggesting that the presence of the drug restricts the availability of Erk to the upstream-activated pathway. Since the population of pShc does not change in response to indomethacin, it is likely that an ancillary, non-receptor tyrosine kinase is responsible for the phosphorylation of Shc. This kinase is up-regulated by the EGF-activated receptor independent of Shc recruitment, but is able to phosphorylate Y317 and hence effect the recruitment of Grb2 to initiate MAPK signalling. A prime candidate for this kinase is Src which has been previously shown to bind to, and phosphorylate Shc on receptor stimulation [41,42] and is known to be expressed in both SkBr3 and A498 cells. Indeed, Shc^{PTB}-independent interactions activate Src family kinases in a subset of breast cancers [43].

In the second mechanism (MCF7, Fig. 5A; A431, Fig. 5C; and HeLa, Fig. 5E) the levels of phosphorylation of all of the components of the MAPK pathway (i.e. Shc, Mek and Erk) are depleted in an indomethacin dose-dependent manner suggesting that the inhibitor is blocking binding to the receptor in a conventional way. For example, in HeLa cells there is a clear correlation in reduction of pShc and pErk. The concomitant reduction in pMek confirms that the entire MAPK pathway is being inhibited. The lack of prolonged elevation of pShc indicates that there is no impact from ancillary kinase activity. The question as to why the different mechanisms prevail in cell lines is likely to be the result of differential protein expression profiles in the cells. In particular, the availability of active non-receptor tyrosine kinase in some cell lines can impact on Shc phosphorylation and drive the MAPK pathway through recruitment of Grb2. However, in all cases the sequestering of Erk from the pathway down-regulates downstream signalling.

Our binding studies indicate that the affinity of indomethacin for

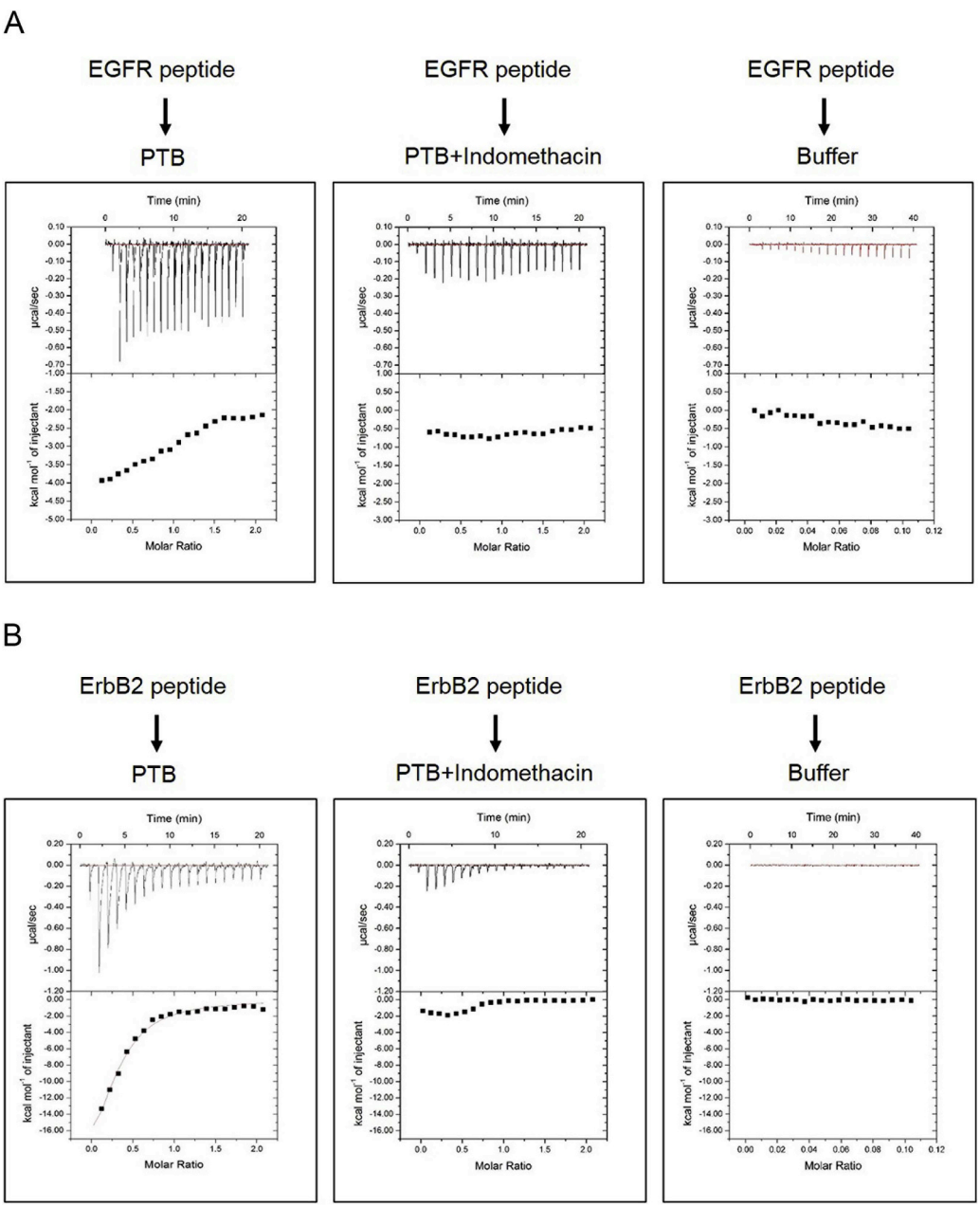

Fig. 4. Binding of indomethacin to Shc^{PTB} reduces the Shc^{PTB}–phosphotyrosine interaction. (**A**) ITC measurement of the interaction between EGFR pY1148 (EGFR peptide: STAVGNPEpYLNT) and Shc^{PTB} in the absence and presence of indomethacin. Left: twenty 2 µl injections of EGFR pY1148 (500 µM) were titrated into Shc^{PTB} (50 µM) at 25 °C. Middle: twenty 2 µl injections of EGFR pY1148 (500 µM) were titrated into 50 µM Shc^{PTB} pre-incubated with 2 mM of Indomethacin at 25 °C. Right: control experiment in which twenty 2 µl injections of EGFR pY1148 (500 µM) were titrated into buffer solution. (**B**) ITC measurement of the interaction between ErbB2 pY1122 (SPAFDNLYpYWDQ) and Shc^{PTB} in the absence and presence of indomethacin. Left: twenty 2 µl injections of ErbB2 pY1122 (500 µM) were titrated into Shc^{PTB} (50 µM) at 25 °C. Middle: twenty 2 µl injections of ErbB2 pY1122 (500 µM) were titrated into 50 µM Shc^{PTB} pre-incubated with 2 mM of indomethacin at 25 °C. Right: Control experiment in which twenty 2 µl injections of EGFR pY1114 (500 µM) were titrated into buffer solution. (**D**) Interaction of indomethacin with Shc^{PTB} is measured using MST. Unlabelled ErbB2 pY1122 (60 µM–1.83 nM) was titrated into a fixed concentration of labelled Shc^{PTB} (50 nM) (red curve). Pre-incubated Shc^{PTB} (50 nM) with 200 µM indomethacin disrupted the interaction to ErbB2 pY1122 peptide (green curve). (For interpretation of the references to colour in this figure legend, the reader is referred to the Web version of this article.)

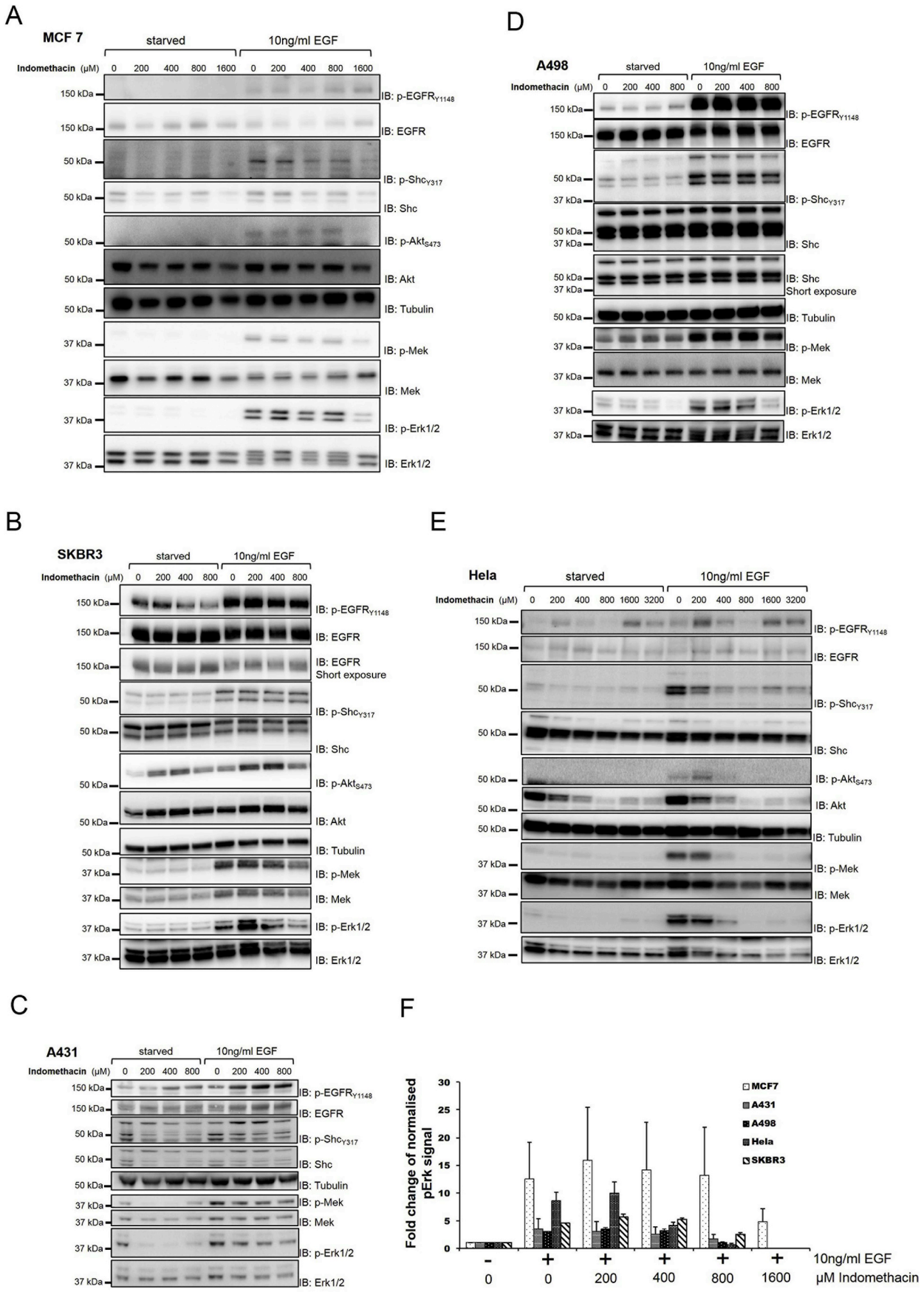

Fig. 5. Indomethacin down-regulates EGF-dependent Erk1/2 pathway in cancer cell lines. The effects of indomethacin in EGFR pathway were examined by immunoblotting. (A) MCF7, (B) SkBr3 (C) A431, (D) A498, and (E) HeLa cells were serum-starved and treated with different concentrations of indomethacin as indicated. After EGFR stimulation cells were lysed and probed with various antibodies to examine the effect of indomethacin on the EGF-dependent pathway. The biphasic nature of EGFR phosphorylation in HeLa cells could result from iatrogenic stress induced, ligand-independent EGFR transactivation.

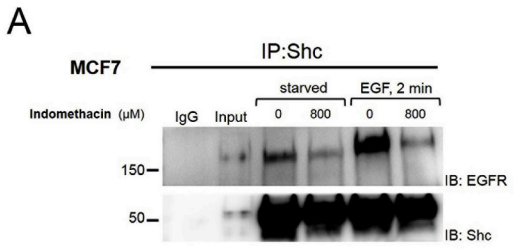

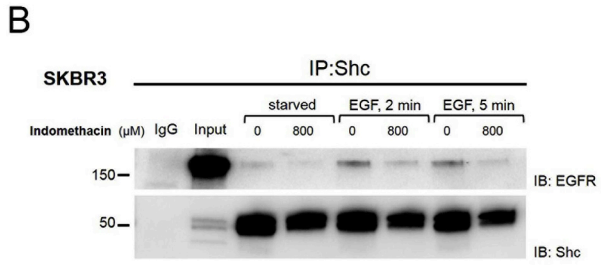

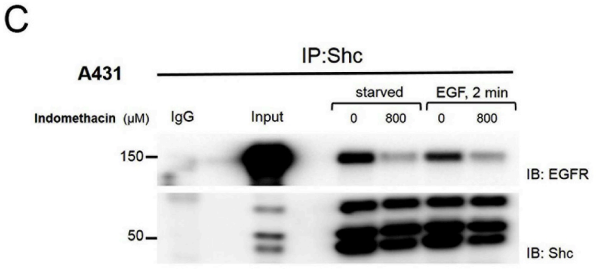

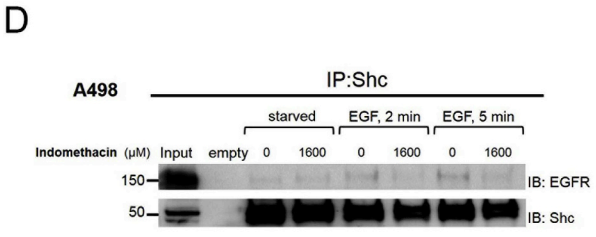

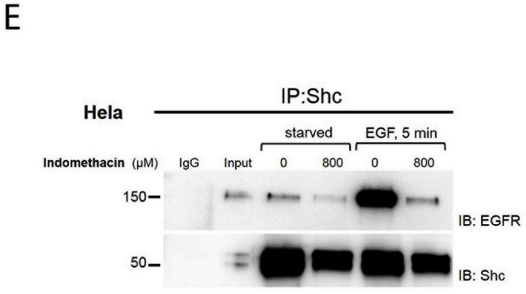

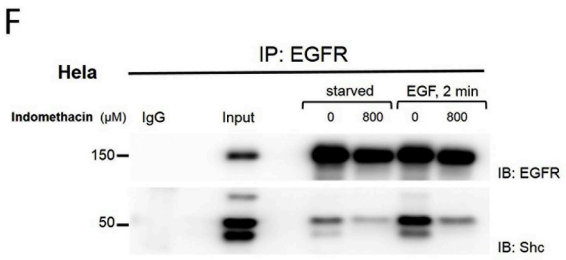

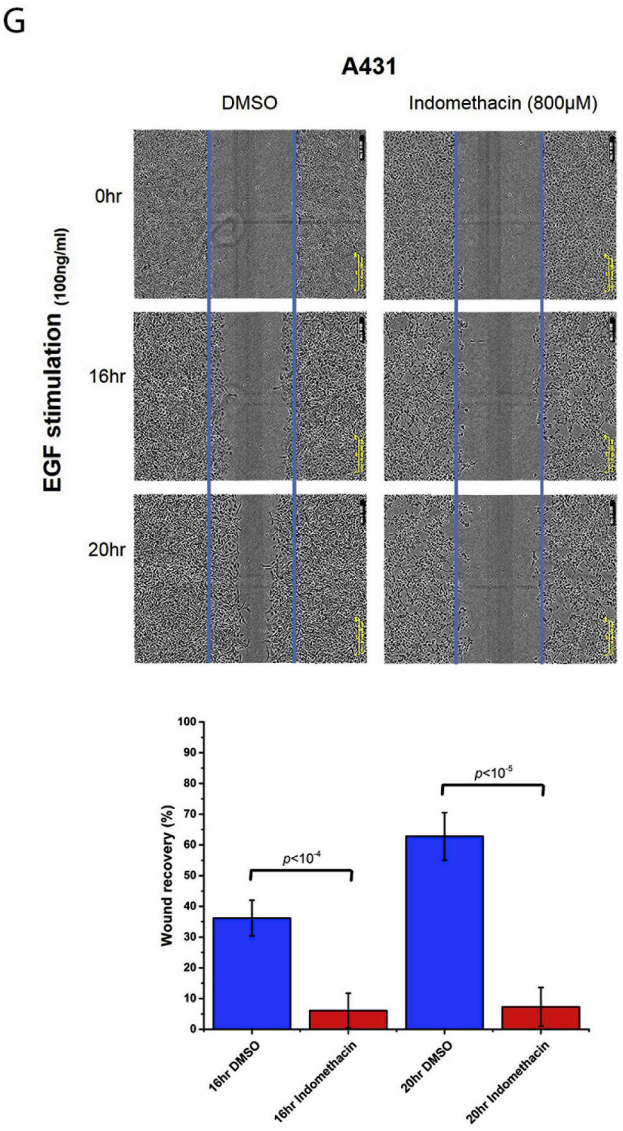

(caption on next page)

Fig. 6. Indomethacin competes with EGFR for binding to Shc. (A) MCF7, (B) SkBr3, (C) A431, (D) A498, and (E) HeLa cells were used to immunoprecipitate Shc and observe the Shc-EGFR complex formation by immunoblotting. Cells were serum-starved and treated with indomethacin (MCF7: 0 μM and 800 μM, SKBR3: 0 μM and 800 μM, A431: 0 μM and 800 μM, A498: 0 μM and 1600 μM, and Hela: 0 μM and 800 μM). After EGFR stimulation cells were lysed and probed for Shc and EGFR, (F) A431 cells were use to immunoprecipitate EGFR and observe the EGFR-Shc complex formation by immunoblotting, and (G) Representative images and quantitative data of a wound healing migration assay in the presence or absence of 800 μM indomethacin for 16 and 20 h.

the PTB domain is significantly tighter than the effective concentration of indomethacin used in cancer cell lines. This common observation in inhibitor studies could result from several sources. For example, the ability of indomethacin to penetrate different cell membranes and the stability of indomethacin once inside the cell.

3.5. Indomethacin competes with EGFR for binding to Shc in cancer cell lines

Finally, having shown that indomethacin inhibits the binding between Shc and EGFR *in vitro* and EGFR-dependent Erk phosphorylation in different cancer cell lines, we sought to establish that the Shc-EGFR interaction is indeed disrupted upon indomethacin treatment. We immunoprecipitated Shc from MCF7, Fig. 6A; SkBr3, Fig. 6B; A431, Fig. 6C; A498, Fig. 6D; and HeLa, Fig. 6E cells in the presence and absence of indomethacin. Also for comparison we immunoprecipitated EGFR from A431 cells in the presence and absence of indomethacin (Fig. 6F). The Shc-mediated complex formation was examined by immunoblotting. Treating cells with indomethacin is shown to apparently block the EGFR-Shc interaction upon EGF stimulation (Fig.s 6A-F). This confirms that indomethacin can compete with the pTyr residues on EGFR for binding to Shc^{PTB}.

One outcome of EGFR-mediated MAPK pathway activation is increased cell motility. Therefore, to confirm the role of indomethacin in the inhibition of Shc-mediated MAPK signalling, we performed a wound-healing assay using A431 cells. Serum-starved A431 cells were stimulated with 100 ng/ml EGF in the presence of 800 μM of indomethacin or the same volume of DMSO (Fig. 6G). The assay clearly demonstrated that the indomethacin treatment inhibits the migratory potential of A431 cells over the time course.

4. Discussion

The MAPK pathway is a key regulator of several important cellular functions such as proliferation, survival and migration. Dysregulation of its upstream components such as RTKs and the small GTPase, Ras is the driver for a range of pathologies including cancer. Numerous studies have focused on exploring the mechanisms of activation of MAPK signalling and regulation to provide therapeutic approaches to block oncogenic signal transduction. Here, we sought a fundamentally novel approach to down-regulate MAPK signalling through inhibition of Shc-mediated activity of Erk by identifying a small molecule inhibitor for the Shc^{PTB}-EGFR interaction. In preventing Shc from binding to activated EGFR, the small molecule can have dual functionality through contributing to reduction of pErk by two distinct mechanisms; 1) stabilising the Shc-Erk complex, and 2) preventing phosphorylation of Shc by the receptor and thus blocking the recruitment of Grb2. *In silico* docking studies directed at Shc^{PTB} revealed a known NSAID, indomethacin, as the best virtual hit. *In vitro* biophysical binding assays confirmed that indomethacin can interact with Shc^{PTB}. NMR spectroscopic analysis indicates that the binding site for indomethacin on PTB is located within the pTyr-binding pocket. Importantly, we did not observe any significant chemical shifts at the Erk binding interface upon indomethacin binding (Fig. 3C) [1]. This indicates that binding indomethacin can block the interaction with the receptor without perturbation of the interaction with Erk. To test our observation in a cellular context, we treated several cancer cell lines with indomethacin and examined its effects on MAPK signal transduction. Evidence of a reduction of pErk was observed which appears to be driven in specific cell types by two distinct mechanisms of a dual function inhibitor.

While indomethacin is commonly used as an anti-inflammatory drug through inhibiting the cyclooxygenases Cox-1 and -2, it has been reported to show some cancer suppressive activities. Inhibition of Cox-2 was revealed to be effective in blocking angiogenesis in tumours, and prodrugs incorporating indomethacin have been used to target cancer cells and block vascular development [44]. Indomethacin has also been shown to reduce cell migration [45] and invasion [46,47], properties associated with cancer progression. Indeed indomethacin appears to be able to interfere with calcium-dependent pathways and focal complexes, which in turn, contribute to blocking cancer cell migration. Furthermore, a number of studies have shown that indomethacin inhibits cell proliferation and augments apoptosis in colorectal cancer cell lines, some of which do not express Cox-1 or -2 [48]. This indicates that such anti-tumour effects are mediated in a Cox-independent manner, at least in some cellular environments. Through our interdisciplinary approach, we have demonstrated that indomethacin competes with activated EGFR for the pTyr-binding pocket in the Shc^{PTB} and in doing so is able to reduce the levels of free Erk leading to depression of MAPK signalling. In this way indomethacin can negatively impact on proliferative outcomes from cells in tumour growth. Interestingly, EGF is a known potent activator of Cox-2 [49], therefore the role of indomethacin highlighted here might also extend to down-regulation of the tumour-associated activity of this protein.

The PTB domain from Shc has been shown to bind to other ligands that can impinge on cancer signalling. One important example is the phosphatase PTP-PEST which is a known binding partner of Shc^{PTB} [50]. Depletion of PTP-PEST in triple negative breast cancer cells leads to hyperactivation of Erk, and its over-expression results in dephosphorylation of EGFR and Shc at Y317 [51]. However, the impact of this negative-regulator of MAPK signalling is likely to be offset in the treatment with high doses of indomethacin. Our data show that at high dosage indomethacin can inhibit the EFGR-Shc^{PTB} interaction which we have shown is of the order of 100 nM. Since the interaction between PTP-PEST is of the order of 10 μM [52] it is likely that the drug would block this interaction at similar dosage. It is thus clear that in some cell lines the effect of indomethacin in inhibition of negative regulators of proliferative signalling would need to be weighed against the modus operandi described herein.

Indomethacin binds at least 100-fold weaker than a pTyr-containing peptide corresponding to the cognate binding site for Shc on EGFR. This makes it unsuitable as a drug for targeting Shc. Nonetheless, our data provide strong validation for an approach that targets the Shc^{PTB} and the resulting sequestering of Erk. It may also suggest the potential for development of indomethacin as a hit compound toward lead generation.

Conflict of interest statement

The authors of this manuscript declare no conflict of interest.

Acknowledgments

This work was funded in part by CRUK grant C57233/A22356. The authors also thank the São Paulo Research Foundation (FAPESP) for funding this project (2013/18009-4).

Molecular graphics and analyses were performed with the UCSF Chimera package. Chimera is developed by the Resource for Biocomputing, Visualization, and Informatics at the University of California, San Francisco (supported by NIGMS P41-GM103311).

Appendix A. Supplementary data

Supplementary data to this article can be found online at https://doi.org/10.1016/j.canlet.2019.05.008.

References

[1] K.M. Suen, C.-C. Lin, R. George, F.A. Melo, E.R. Biggs, Z. Ahmed, M.N. Drake, S. Arur, S.T. Arold, J.E. Ladbury, Interaction with Shc prevents aberrant Erk activation in the absence of extracellular stimuli, Nat. Struct. Mol. Biol. 20 (2013) 620–627.

[2] E. Mercalli, S. Ghizzoni, E. Arighi, L. Alberti, R. Sangregorio, M.T. Radice, M.L. Gishizky, M.A. Pierotti, M.G. Borrello, Key role of Shc signaling in the transforming pathway triggered by Ret/ptc2 oncoprotein, Oncogene 20 (2001) 3475–3485.

[3] M. Rajendran, P. Thomes, L. Zhang, S. Veeramani, M.F. Lin, p66Shc–a longevity redox protein in human prostate cancer progression and metastasis: p66Shc in cancer progression and metastasis, Cancer Metastasis Rev. 29 (2010) 207–222.

[4] P. van der Geer, S. Wiley, G.D. Gish, T. Pawson, The Shc adaptor protein is highly phosphorylated at conserved, twin tyrosine residues (Y239/240) that mediate protein-protein interactions, Curr. Biol. 6 (1996) 1435–1444.

[5] K.S. Ravichandran, M.M. Zhou, J.C. Pratt, J.E. Harlan, S.F. Walk, S.W. Fesik, S.J. Burakoff, Evidence for a requirement for both phospholipid and phosphotyrosine binding via the Shc phosphotyrosine-binding domain in vivo, Mol. Cell. Biol. 17 (1997) 5540–5549.

[6] D.T. Sweet, E. Tzima, Spatial signaling networks converge at the adaptor protein Shc, Cell Cycle 8 (2009) 231–235.

[7] M.M. Zhou, K.S. Ravichandran, E.F. Olejniczak, A.M. Petros, R.P. Meadows, M. Sattler, J.E. Harlan, W.S. Wade, S.J. Burakoff, S.W. Fesik, Structure and ligand recognition of the phosphotyrosine binding domain of Shc, Nature 378 (1995) 584–592.

[8] M.M. Zhou, B. Huang, E.T. Olejniczak, R.P. Meadows, S.B. Shuker, M. Miyazaki, T. Trüb, S.E. Shoelson, S.W. Fesik, Structural basis for IL-4 receptor phosphopeptide recognition by the IRS-1 PTB domain, Nat. Struct. Biol. 3 (1996) 388–393.

[9] K.S. Yan, M. Kuti, S. Yan, S. Mujtaba, A. Farooq, M.P. Goldfarb, M.M. Zhou, FRS2 PTB domain conformation regulates interactions with divergent neurotrophic receptors, J. Biol. Chem. 277 (2002) 17088–17094.

[10] L. Zeng, M. Kuti, S. Mujtaba, M.M. Zhou, Structural insights into FRS2α PTB domain recognition by neurotrophin receptor TrkB, Proteins 82 (2014) 1534–1541.

[11] R. George, A.C. Schuller, R. Harris, J.E. Ladbury, A phosphorylation-dependent gating mechanism controls the SH2 domain interactions of the Shc adaptor protein, J. Mol. Biol. 377 (2008) 740–747.

[12] J. Ursini-Siegel, W.R. Hardy, Y. Zheng, C. Ling, D. Zuo, C. Zhang, L. Podmore, T. Pawson, W.J. MulleR, The ShcA SH2 domain engages a 14-3-3/PI3'K signaling complex and promotes breast cancer cell survival, Oncogene 31 (2012) 5038–5044.

[13] T.P. Garrington, G.L. Johnson, Organization and regulation of mitogen-activated protein kinase signaling pathways, Curr. Opin. Cell Biol. 11 (1999) 211–218.

[14] W. Kolch, Coordinating ERK/MAPK signalling through scaffolds and inhibitors, Nat. Rev. Mol. Cell Biol. 6 (2005) 827–837.

[15] R. Steinmetz, H.A. Wagoner, P. Zeng, J.R. Hammond, T.S. Hannon, J.L. Meyers, O.H. PescovitZ, Mechanisms regulating the constitutive activation of the extracellular signal-regulated kinase (ERK) signaling pathway in ovarian cancer and the effect of ribonucleic acid interference for ERK1/2 on cancer cell proliferation, Mol. Endocrinol. 18 (2004) 2570–2582.

[16] D.T. Price, G. Della Rocca, C. Guo, M.S. Ballo, D.A. Schwinn, L.M. Luttrell, Activation of extracellular signal-regulated kinase in human prostate cancer, J. Urol. 162 (1999) 1537–1542.

[17] J. Zheng, D.J. Son, H.L. Lee, H.P. Lee, T.H. Kim, J.H. Joo, Y.W. Ham, W.J. Kim, J.K. Jung, S.B. Han, J.T. Hong, (E)-2-methoxy-4-(3-(4-methoxyphenyl)prop-1-en-1-yl)phenol suppresses ovarian cancer cell growth via inhibition of ERK and STAT3, Mol. Carcinog. 56 (2017) 2003–2013.

[18] S. Yoon, R. Seger, The extracellular signal-regulated kinase: multiple substrates regulate diverse cellular functions, Growth Factors 24 (2006) 21–44.

[19] S. Arur, M. Ohmachi, S. Nayak, M. Hayes, A. Miranda, A. Hay, A. Golden, T. Schedl, Multiple ERK substrates execute single biological processes in Caenorhabditis elegans germ-line development, Proc. Natl. Acad. Sci. U.S.A. 106 (2009) 4776–4781.

[20] S.M. Carlson, C.R. Chouinard, A. Labadorf, C.J. Lam, K. Schmelzle, E. Fraenkel, F.M. White, Large-scale discovery of ERK2 substrates identifies ERK-mediated transcriptional regulation by ETV3, Sci. Signal. 4 (2011) rs11.

[21] A.V. Khokhlatchev, B. Canagarajah, J. Wilsbacher, M. Robinson, M. Atkinson, E. Goldsmith, M.H. Cobb, Phosphorylation of the MAP kinase ERK2 promotes its homodimerization and nuclear translocation, Cell 93 (1998) 605–615.

[22] M.K. Dougherty, J. Müller, D.A. Ritt, M. Zhou, X.Z. Zhou, T.D. Copeland, T. P Conrads, T.D. Veenstra, K.P. Lu, D.K. Morrison, Regulation of Raf-1 by direct feedback phosphorylation, Mol. Cell 17 (2005) 215–224.

[23] M.C. Mendoza, E.E. Er, J. Blenis, The Ras-Erk and PI3K-mTOR pathways: cross-talk and compensation, Trends Biochem. Sci. 36 (2011) 320–328.

[24] K.M. Suen, C.-C. Lin, C. Seiler, R. George, G. Poncet-Montange, A.B. Biter, Z. Ahmed, S.T. Arold, J.E. Ladbury, Phosphorylation of threonine residues on Shc promotes ligand binding and mediates crosstalk betweem MAPK and Akt pathways in breast cancer, Int. J. Biochem. Cell Biol. 94 (2018) 89–97.

[25] R. Ahn, V. Sabourin, J.R. Ha, S. Cory, G. Maric, Y.K. Im, W.R. Hardy, H. Zhao, M. Park, M. Hallett, P.M. Siegel, T. Pawson, J. Ursini-Siegel, The ShcA PTB domain functions as a biological sensor of phosphotyrosine signaling during breast cancer progression, Cancer Res. 73 (2013) 4521–4532.

[26] D.S. Wishart, Y.D. Feunang, A.C. Guo, E.J. Lo, A. Marcu, J.R. Grant, T. Sajed, D. Johnson, C. Li, Z. Sayeeda, N. Assempour, I. Iynkkaran, Y. Liu, A. Maciejewski, N. Gale, A. Wilson, L. Chin, R. Cummings, D. Le, A. Pon, C. Knox, M. Wilson, DrugBank 5.0: a major update to the DrugBank database for 2018, Nucleic Acids Res. 46 (2018) D1074–D1082.

[27] P.C. Hawkins, A.G. Skillman, G.L. Warren, B.A. Ellingson, M.T. Stahl, Conformer generation with OMEGA: algorithm and validation using high quality structures from the Protein Databank and Cambridge Structural Database, J. Chem. Inf. Model. 50 (2010) 572–584.

[28] M. McGann, FRED pose prediction and virtual screening accuracy, J. Chem. Inf. Model. 51 (2011) 578–596.

[29] M. McGann, FRED and HYBRID docking performance on standardized datasets, J. Comput. Aided Mol. Des. 26 (2012) 897–906.

[30] B.P. Kelley, S.P. Brown, G.L. Warren, S.W. Muchmore, POSIT: flexible shape-guided docking for pose prediction, J. Chem. Inf. Model. 55 (2015) 1771–1780.

[31] E.F. Pettersen, T.D. Goddard, C.C. Huang, G.S. Couch, D.M. Greenblatt, E.C. Meng, T.E. Ferrin, UCSF Chimera–a visualization system for exploratory research and analysis, J. Comput. Chem. 25 (2004) 1605–1612.

[32] K. Stierand, P.C. Maass, M. Rarey, Molecular complexes at a glance: automated generation of two-dimensional complex diagrams, Bioinformatics 22 (2006) 1710-1706.

[33] E. Lescop, P. Schanda, B. Brutscher, A set of BEST triple-resonance experiments for time-optimized protein resonance assignment, J. Magn. Reson. 187 (2007) 163–169.

[34] T. Schulte-Herbrüggen, O. Sørensen, Clean TROSY: compensation for relaxation-induced artifacts, J. Magn. Reson. 144 (2000) 123–128.

[35] K. Pervushin, R. Riek, G. Wider, K. Wüthrich, Attenuated T2 relaxation by mutual cancellation of dipole–dipole coupling and chemical shift anisotropy indicates an avenue to NMR structures of very large biological macromolecules in solution, Proc. Natl. Acad. Sci. Unit. States Am. 94 (1997) 12366–12371.

[36] F. Delaglio, S. Grzesiek, G.W. Vuister, G. Zhu, J. Pfeifer, A. Bax, NMRPipe: a multidimensional spectral processing system based on UNIX pipes, J. Biomol. NMR 6 (1995) 277–293.

[37] W.F. Vranken, W. Boucher, T.J. Stevens, R.H. Fogh, A. Pajon, M. Llinas, E.L. Ulrich, J.L. Markley, J. Ionides, E.D. Laue, The CCPN data model for NMR spectroscopy: development of a software pipeline, Proteins 59 (2005) 687–696.

[38] M.M. Zhou, J.E. Harlan, W.S. Wade, S. Crosby, K.S. Ravichandran, S.J. Burakoff, S.W. Fesik, Binding affinities of tyrosine-phosphorylated peptides to the COOH-terminal SH2 and NH-terminal phosphotyrosine binding domains of Shc, J. Biol. Chem. 270 (1996) 31119–31123.

[39] M. Offterdinger, V. Georget, A. Girod, P.I.H. Bastiaens, Imaging phosphorylation dynamics of the epidermal growth factor receptor, J. Biol. Chem. 279 (2004) 36972–36981.

[40] M.J. Smith, W.R. Hardy, J.M. Murphy, N. Jones, T. Pawson, Screening for PTB domain binding partners and ligand specificity using proteome-derived NPXY peptide arrays, Mol. Cell. Biol. 26 (2006) 8461–8474.

[41] J. McGlad, A. Cheng, G. Pelicci, P.G. Pelicci, T. Pawson, Shc proteins are phosphorylated and regulated by the v-Src and v-Fps protein-tyrosine kinases, Proc. Natl. Acad. Sci. U.S.A. 89 (1992) 8869–8873.

[42] A.C. Schüller, Z. Ahmed, J.A. Levitt, K.M. Suen, K. Suhling, J.E. Ladbury, Indirect recruitment of the signalling adaptor Shc to the fibroblast growth factor receptor 2 (FGFR2), Biochem. J. 416 (2008) 189–199.

[43] J.R. Ha, R. Ahn, H.W. Smith, V. Sabourin, S. Hébert, E.C. Cañedo, Y.K. Im, C.L. Kleinman, W.J. Muller, J. Ursini-Siegel, Integration of distinct ShcA signaling complexes promotes breast tumor growth and tyrosine kinase inhibitor resistance, Mol. Cancer Res. 16 (2018) 894–908.

[44] K.S. Kim, A. Sharma, W.X. Ren, J. Han, J.S. Kim, COX-2 Inhibition mediated anti-angiogenic activatable prodrug potentiates cancer therapy in preclinical models, Biomaterials 185 (2018) 63–72.

[45] G. Guo, C.E. Ott, J. Grünhagen, B. Muñoz-García, A. Pletschacher, K. Kallenbach, Y. von Kodolitsch, P.N. Robinson, Indomethacin prevents the progression of thoracic aortic aneurysm in Marfan syndrome mice, Aorta (Stamford) 1 (2013) 5–12.

[46] H.M. Wang, G.Y. Zhang, Indomethacin suppresses growth of colon cancer via inhibition of angiogenesis in vivo, World J. Gastroenterol. 11 (2005) 340–343.

[47] E. Ackerstaff, B. Gimi, D. Artemov, Z.M. Bhujwalla, Anti-inflammatory agent indomethacin reduces invasion and alters metabolism in a human breast cancer cell line, Neoplasia 9 (2007) 222–235.

[48] M.A. Hull, S.H. Gardner, G. Hawcroft, Activity of the non-steroidal anti-inflammatory drug indomethacin against colorectal cancer, Cancer Treat Rev. 29 (2003) 309–320.

[49] S. Kulkarni, J.S. Rader, F. Zhang, H. Liapis, A.T. Koki, J.L. Masferrer, K. Subbaramaiah, A.J. Dannenberg, Cyclooxygenase-2 is overexpressed in human cervical cancer, Clin. Cancer Res. 7 (2001) 429–434.

[50] A. Charest, J. Wagner, S. Jacob, C.J. McGlade, M.L. Tremblay, Phosphotyrosine-independent binding of SHC to the NPLH sequence of murine protein-tyrosine phosphatase-PEST, J. Biol. Chem. 271 (1996) 8424–8429.

[51] T. Sun, N. Aceto, K.L. Meerbrey, J.D. Kessler, C. Zhou, I. Migliaccio, D.X. Nguyen, N.N. Pavlova, M. Botero, J. Huang, R.J. Bernardi, E. Schmitt, G. Hu, M.Z. Li, N. Dephoure, S.P. Gygi, M. Rao, C.J. Creighton, S.G. Hilsenbeck, C.A. Shaw, D. Muzny, R.A. Gibbs, D.A. Wheeler, C.K. Osborne, R. Schiff, M. Bentires-Alj, S.J. Elledge, T.F. Westbrook, Activation of multiple proto-oncogenic tyrosine kinases in breast cancer via loss of the PTPN12 phosphatase, Cell 144 (2011) 703–718.

[52] M.J. Smith, W.R. Hardy, G.Y. Li, M. Goudreault, S. Hersch, P. Metalnikov, A. Starostine, T. Pawson, M. Ikura, The PTB domain of ShcA couples receptor activation to the cytoskeletal regulator IQGAP1, EMBO J. 29 (2010) 884–896.